Chapter 4

The Air-Bearing Model

The purpose of this chapter is to achieve a model for the air-cushion conveyor air-bearing. This model will be used in the static design of the air-cushion conveyor. The expressions relate parameters as fluid thickness, load pressure, supply pressure, drag force, temperature rise, flow and orifice diameter.

Fluid Mechanics theory can be used to obtain the parameters that govern the flow under the belt. To avoid starting from scratch, the approach adopted use a reference in Hydrostatic Lubrication, where the principles are similar.

> Hydrostatic lubrication consists in pushing a fluid between the surfaces of a kinematic pair by means of an external pressurization system (...) the pressurized field allows the lift and the bearing of the moving member on the fixed member of the pair. [2]

In the air-cushion conveyor the load is carried in one direction and the radius of curvature of the support is negligible compared to the fluid thickness. This fits with the rectangular pad hydrostatic bearing, which was found to be the most adequate as a reference to model the air flow.

4.1 Hydrostatic Lubrication Principle

Fig. (4.1) contains an outline of the principle of hydrostatic lubrication.

> The recess (of which the projected area is A) of the bearing pad (2) of the pair is fed by a pump; the bearing runner (1) is loaded by a

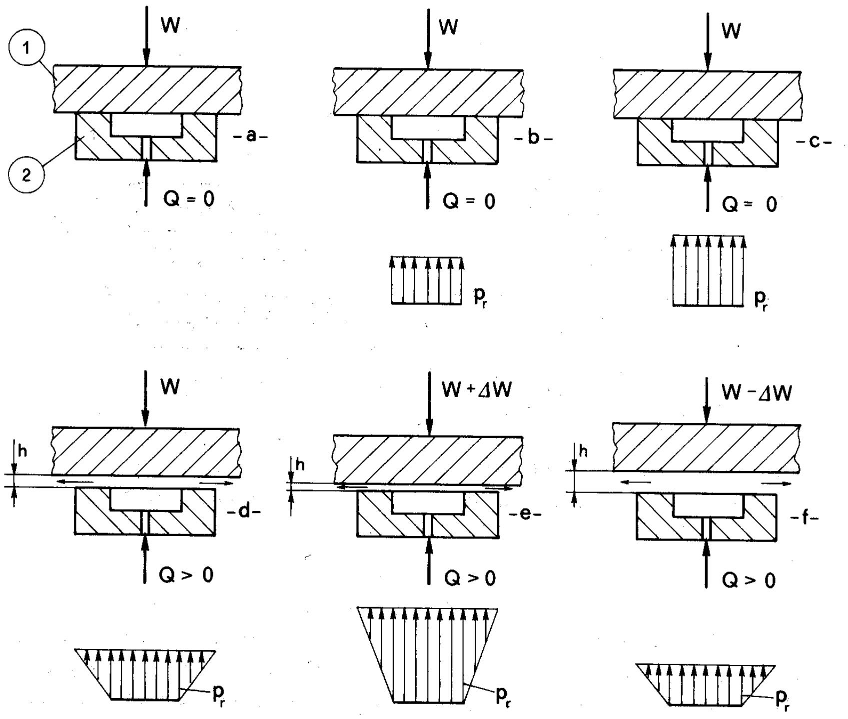

Figure 4.1: Hydrostatic lubrication principle

force W, Fig. (4.1.a). When the pump begins to run, the pressure in the recess grows, Fig. (4.1.b), until the "lifting pressure" $p = W/A$ is reached Fig. (4.1.c); at this point member (1) is lifted, a lubricant film builds up to separate the surfaces, and a flow Q is delivered, due to the pressure step along the clearance Fig. (4.1.d). Different loads lead to different values of the recess pressure and of the film thickness h Fig. (4.1.e) and (4.1.f). [2]

4.2 Flow and Pressure Stability

In order to avoid contact between belt and support it is necessary to maintain a minimum fluid thickness. The flow and pressure under the belt must be controlled to meet this requirement when the bearing is subjected to load disturbances. The kind of supply system and the bearing configuration chosen with care can provide the necessary stability.

4.2.1 Constant Pressure Supply

To have a regular flow trough the orifices it is not practical to use a constant-flow supply system, due to the large amount of orifices. An alternative is the constant-pressure supply. The air is provided by a single pump and distributed to all the orifices by ducts, but in each orifice the flow needs to be controlled by valves or restrictors.

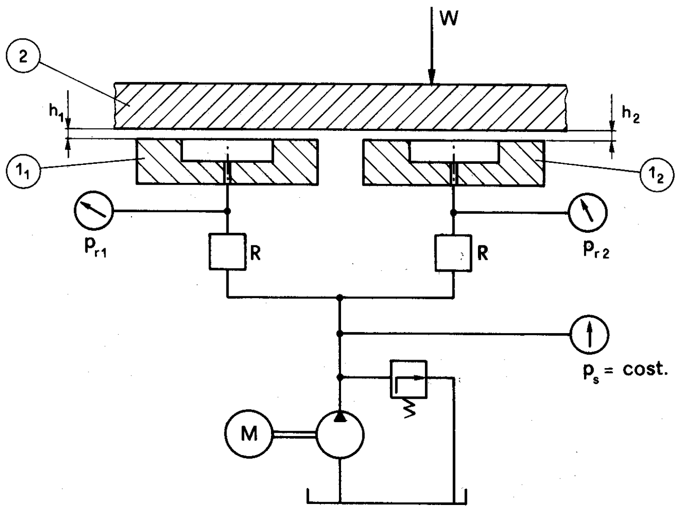

Figure 4.2: Bearing pad with two recesses and a constant pressure supply

4.2.2 Flow Stability

Pressure, flow, load and fluid thickness are related parameters. The pressure in the clearance is determined by the load, while flow and fluid thickness depend on this pressure. A load fluctuation will therefore change the flow and fluid thickness.

To control the flow a valve can be placed in each orifice. A more practical solution is to make the orifices with such a diameter that the flow is controlled automatically for fluid thickness or load disturbances.

The orifices can be drilled with a certain diameter so that the ratio β between clearance pressure p and supply pressure p_s is $\beta = p/p_s < 1$. In this condition, an increase in load, decreasing the fluid film thickness, will decrease the flow in the orifice. The pressure loss in the orifice will therefore decrease. In the limit $h \to 0 \Longrightarrow p \to p_s$.

The ratio β is chosen taking in consideration the expected overload. The value $\beta = 0.5$ provides a non-null fluid film thickness for overloads until $\sim$ 95% of the nominal load pressure.

4.3 Flow in the Clearance

The fluid flow below the belt can be modeled starting with the Navier-Stokes equations. Further assumptions simplify the model to the Reynolds equations. The velocity field is obtained integrating the Reynolds equations, getting expressions depending on the differentials $\partial p/\partial x$ and $\partial p/\partial z$. Viscous stress and flow are derived directly from the velocity field.

4.3.1 Navier-Stokes Equations

Navier-Stokes equations are deduced from the momentum equation (balance of forces) and fluid constitutive relations. The general form of these equations for rectangular coordinates is:

$$\begin{cases} \rho\frac{Du}{Dt} = \rho X - \frac{\partial p}{\partial x} + \frac{\partial}{\partial x}[2\mu(\frac{\partial u}{\partial x} - \frac{1}{3}\nabla\mathbf{v})] + \frac{\partial}{\partial y}[\mu(\frac{\partial u}{\partial y} + \frac{\partial v}{\partial x})] + \frac{\partial}{\partial z}[\mu(\frac{\partial u}{\partial z} + \frac{\partial w}{\partial x})] \\ \rho\frac{Du}{Dt} = \rho Y - \frac{\partial p}{\partial y} + \frac{\partial}{\partial y}[2\mu(\frac{\partial v}{\partial y} - \frac{1}{3}\nabla\mathbf{v})] + \frac{\partial}{\partial z}[\mu(\frac{\partial v}{\partial z} + \frac{\partial w}{\partial y})] + \frac{\partial}{\partial x}[\mu(\frac{\partial u}{\partial y} + \frac{\partial v}{\partial x})] \\ \rho\frac{Du}{Dt} = \rho Z - \frac{\partial p}{\partial z} + \frac{\partial}{\partial z}[2\mu(\frac{\partial w}{\partial z} - \frac{1}{3}\nabla\mathbf{v})] + \frac{\partial}{\partial x}[\mu(\frac{\partial u}{\partial z} + \frac{\partial w}{\partial x})] + \frac{\partial}{\partial y}[\mu(\frac{\partial v}{\partial z} + \frac{\partial w}{\partial y})] \end{cases} \tag{4.1}$$

where ρ is the density of the fluid; μ the viscosity; u, v, w are the components of the velocity vector $\mathbf{v}$ and X, Y, Z the components of the resultant body force.

4.3.2 Continuity Equation

The continuity equation, or the principle of mass conservation, for fluid flow is stated with the equation:

$$\dot{\rho} + \frac{\partial}{\partial x}(\rho u) + \frac{\partial}{\partial y}(\rho v) + \frac{\partial}{\partial z}(\rho w) = 0 \tag{4.2}$$

If density is considered to be constant (relatively small temperature and pressure variations; low Mach number), this equation becomes:

$$\frac{\partial u}{\partial x} + \frac{\partial v}{\partial y} + \frac{\partial w}{\partial z} = 0 \tag{4.3}$$

or in compact form:

$$\nabla \mathbf{v} = 0 \tag{4.4}$$

4.3.3 Reynolds Equations

Due to the fluid film thickness magnitude, compared with belt width, the flow in the clearance can be approximated by the flow between infinite parallel plates, where Reynolds equations may provide satisfactory results for the velocity field.

The Reynolds assumptions are:

- the thickness of the fluid film (in the y direction) is small compared to its size in the other directions (the fluid thickness is in the millimeter order, ~ 1000 times lower than the belt width);
- consequently the pressure, the density and viscosity can be averaged: $\partial p/\partial y = 0$, $\partial \rho/\partial y = 0$, $\partial \mu/\partial y = 0$;
- compared with $\partial u/\partial y$ and $\partial w/\partial y$ all the other velocity gradients are negligible. (This may be a reasonable approximation in the clearance but not in the orifice exit where the flow along y is essential);
- the flow is laminar. No turbulence or vortex exist. (The Reynolds number $Re = \frac{\rho U h}{\mu}$ must be lower than $\sim 2300 Re$).
- the body forces and the inertia terms are negligible compared with the viscous forces.(Air density is relatively low, therefore air weight and inertia are also small)
- the velocity of the fluid in the surfaces coincide with the surface velocity. (This is an usual assumption in viscous fluid flow)

In a developed flow and with the assumptions above, the Navier-Stokes equations are simplified to the Reynolds equations:

$$\begin{cases} \rho\frac{\partial p}{\partial x} = \mu\frac{\partial^2 u}{\partial^2 y} \\ \rho\frac{\partial p}{\partial z} = \mu\frac{\partial^2 w}{\partial^2 y} \end{cases} \tag{4.5}$$

4.3.4 Velocity Field, Flow Rate and Friction

Integrating the Reynolds equations, with boundary conditions $u = 0$ for $y = 0$ and $u = U$ for $y = h$ the components of fluid velocity are:

$$u = \frac{1}{2\mu}\frac{\partial p}{\partial x}y(y-h) + \frac{y}{h}U \tag{4.6}$$

and

$$w = \frac{1}{2\mu}\frac{\partial p}{\partial z}y(y-h) \tag{4.7}$$

The flows in the x and z directions are obtained integrating the velocity in their normal areas. The flow along the x direction, per unit length $\triangle z$ is:

$$q_x = -\frac{h^3}{12\mu}\frac{\partial p}{\partial x} + \frac{h}{2}U \tag{4.8}$$

In the z direction, per unit length $\triangle x$:

$$q_z = -\frac{h^3}{12\mu}\frac{\partial p}{\partial z} \tag{4.9}$$

The Newton formulas for the shear stress are:

$$\tau_x = \mu\frac{\partial u}{\partial y} = \frac{1}{2}\frac{\partial p}{\partial x}(2y-h) + \frac{\mu}{h}U \tag{4.10}$$

$$\tau_z = \mu\frac{\partial w}{\partial y} = \frac{1}{2}\frac{\partial p}{\partial z}(2y-h) \tag{4.11}$$

In the surfaces the shear is:

$$\tau_x = \mp\frac{h}{2}\frac{\partial p}{\partial x} + \frac{\mu}{h}U \tag{4.12}$$

$$\tau_z = \mp\frac{h}{2}\frac{\partial p}{\partial z} \tag{4.13}$$

where the upper sign refers to the $y = 0$ surface and the lower to $y = h$.

Considering $\partial p/\partial x \approx 0$ (infinite length), equation (4.12) becomes:

$$\tau_x = \frac{\mu}{h} U \tag{4.14}$$

The total drag force in the x direction:

$$F_f = \iint_A \pm \tau_x \, dA = \pm \iint_A \left(\frac{\mu}{h} U \right) dx \, dz \tag{4.15}$$

4.4 Flow and Pressure Loss in the Orifices

> In the orifice the Reynolds number often has a high value and the flow becomes "turbulent." [2]

In the case of an orifice with non-negligible length l the flow is given by:

$$Q_i = C_d \frac{\pi d^2}{4} \sqrt{\frac{2}{\rho}(p_s - p)} \tag{4.16}$$

The "discharge coefficient" C_d is given by:

$$C_d = \left(1.5 + 13.74 \sqrt{\frac{l}{dRe}} \right)^{-1/2} \qquad \text{for} \frac{dRe}{l} > 50 \tag{4.17}$$

$$C_d = \left(2.28 + 64 \frac{l}{dRe} \right)^{-1/2} \qquad \text{for} \frac{dRe}{l} < 50 \tag{4.18}$$

Defining the Reynolds number as:

$$Re = \frac{\rho \overline{v} d}{\mu} = \frac{4 Q_i \rho}{\mu \pi d} \tag{4.19}$$

This implies that the coefficient C_d is not directly dependent on the diameter:

$$C_d = \left(1.5 + 13.74 \sqrt{\frac{\mu \pi l}{4 Q_i \rho}} \right)^{-1/2} \qquad \text{for} \frac{Q_i \rho}{\mu \pi l} > 12.5 \tag{4.20}$$

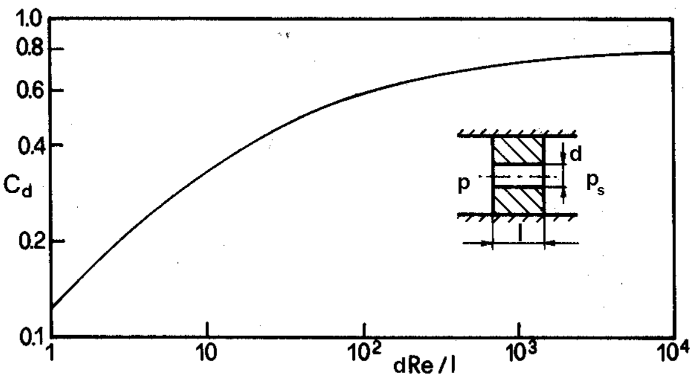

Figure 4.3: Discharge coefficient for a short tube orifice

$$C_d = \left(2.28 + 64\frac{\mu\pi l}{4Q_i\rho}\right)^{-1/2} \qquad \text{for} \frac{Q_i\rho}{\mu\pi l} < 12.5 \tag{4.21}$$

Expression (4.16) can be used to derive the diameter d of the central orifices if the tube length l and the required flow Q_i are given:

$$d = \sqrt{\frac{4}{\pi C_d} Q_i \left(\frac{\rho}{2(p_s - p)}\right)^{1/2}} \tag{4.22}$$

4.5 Bearing Coefficients

The power needed to push lubricant H_p:

$$H_p = p_s Q_t \tag{4.23}$$

where p_s is the supply pressure and Q_t the total flow.

The power dissipated due to the relative velocity between the surfaces H_f:

$$H_f = F_f U \tag{4.24}$$

Assuming that all the dissipated power remains in the lubricant the temperature rise $\triangle T$ is:

$$\triangle T = \frac{H_p + H_f}{Q_t c_p \rho} \tag{4.25}$$

c_p is the specific heat of air.

Pressure ratio β:

$$\beta = \frac{p_{max}}{p_s} \tag{4.26}$$

The term p_{max} is the maximum load pressure in the reference configuration.

4.6 Static Response to Overloads

As load increases and h tends to be smaller, the flow will decrease. Consequently the orifice exit pressure will increase compensating for the load excess. This occurs simultaneously with an increase in stiffness.

The expression that relates h with the additional load ratio W/W_0 is:

$$\frac{h}{h_0} = \sqrt[6]{\frac{1 - \beta W/W_0}{(1-\beta)(W/W_0)^2}} \tag{4.27}$$

In figure (4.4.a) this relation is plotted for several values of β. The curves describe the fluid film thickness variation with load. Increasing loads decrease fluid thickness. For lower values of pressure ratio β the air-bearing withstands higher overloads.

In figure (4.4.b) the bearing stiffness is plotted against the overload ratio, for several pressure ratios. The lower the pressure ratio is the stiffer is the bearing. The shape of the curves show that the stiffness increase with increasing load until certain point and then decreases.

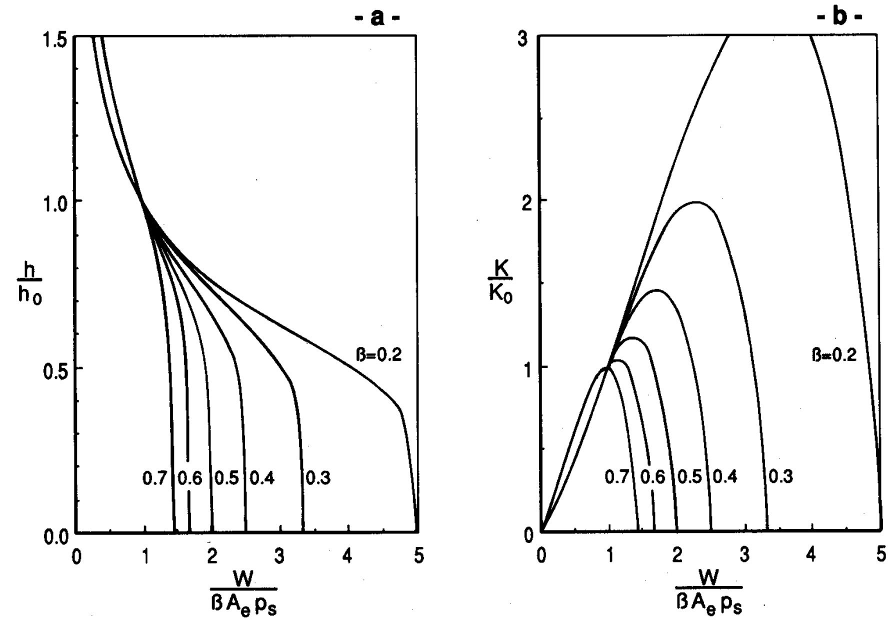

Figure 4.4: Orifice compensation: clearance height (a) and stiffness (b) versus load

Chapter 5

Design Parameters

The procedures here described will be used to obtain the parameters of an air-cushion conveyor: resistances, tensions, support geometry and thickness, drive and pumping power, flow and temperature rise.

So far there are no standard procedures to design an air-supported belt conveyor. The method adopted in this chapter is basically a combination of procedures used to design a troughed belt conveyor and an hydrostatic bearing.

5.1 Design Procedures

The adopted procedure consist in the following steps:

1. Identification and/or specification of initial parameters.
2. Belt selection.
3. Choice of conveyor configuration and location of the most relevant elements.
4. Calculation of the main resistances and tensions on the belt.
5. Sketch of the support structure.
6. Calculation of pumping and drive power

5.2 Initial Parameters

The parameters that come directly from the specifications are:

- conveyor length L $[m]$
- belt capacity C $[Kg/s]$
- bulk material density ρ_{bulk} $[Kg/m^3]$
- height of lift or fall of the load H $[m]$

The following parameters do not belong necessarily to specifications but must be stipulated *a priori*:

- belt width B $[m]$
- belt resistance R $[N/m]$
- belt thickness $t_{belt}[m]$
- belt density $\rho_{belt}[Kg/m^3]$
- fluid film thickness h_r and/or $h_c[m]$
- belt velocity U $[m/s]$
- fluid properties: viscosity μ $[Ns/m^2]$ and density ρ $[Kg/m^3]$
- scrapers normal force F_{scr1} and F_{scr2} $[N/m]$
- friction coefficients between scrapers and belt μ_{bs1} and μ_{bs2}
- support material yield strength $S_y[Pa]$
- safety factors for the support n_l (load) and n_s (material)
- overload ratio W/W_0
- pressure ratio $\beta = p_{max}/p_s$
- drive pulley friction factor μ_p
- drive pulley angle of contact θ_p

If at the end of the pre-design process the results are not suitable, the procedures must be repeated from this point.

5.3 Configuration

The configuration of conveyors depend on the lift or fall of the load and in the last case if the load is regenerative. If there is no fall or lift the adopted configuration is as for the inclined conveyor. In all cases the following elements will be considered:

- Belt and Support Structure
- Fans
- Head, Tail and Drive Pulleys
- Take-up device
- Turnovers
- Scrapers

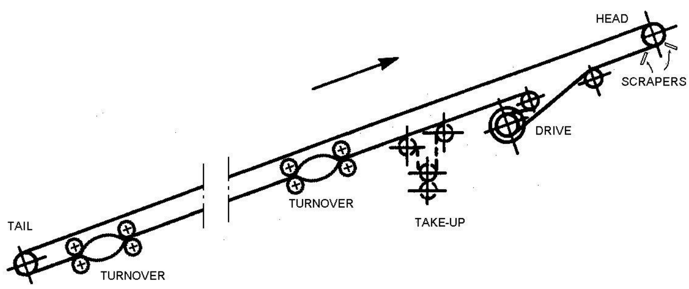

Figure 5.1: Inclined conveyor

5.4 Main Resistances and Tensions

The main resistances are the force to accelerate the bulk material in the loading zone, the viscous drag force, the return side idler friction, the tangential component of the weight (belt+bulk material) and the dry friction in the scrapers. The viscous drag forces are:

$$F_c = \frac{\mu}{h_c} ULB \tag{5.1}$$

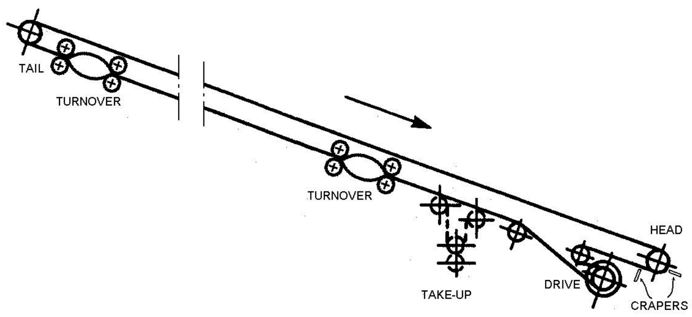

Figure 5.2: Declined conveyor

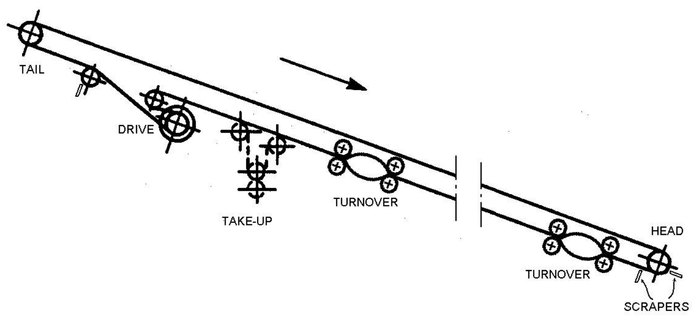

Figure 5.3: Declined conveyor with regenerative load

in the carrying side, and:

$$F_r = \frac{\mu}{h_r} ULB \tag{5.2}$$

in the return side. The parameters h_c and h_r stand for fluid film thickness.

Considering idlers in the return side, the alternative expression for F_r is:

$$F_r = f_e \times Q \times L \times g \tag{5.3}$$

f_e - equipment friction factor
$Q[kg/m]$ - mass of moving parts

If the required power to accelerate the bulk material is provided by the belt, this will be translated in an additional resistance, given by:

$$F_b = CU \tag{5.4}$$

The resultant from the dry friction forces caused by the primary and secondary scrapers placed on the head end is:

$$F_s = F_{scr1}\mu_{bs1}B + F_{scr2}\mu_{bs2}B \tag{5.5}$$

whereF_{scr1} and F_{scr2} are the normal forces on the belt, μ_{bs1} and μ_{bs2} the coefficients of friction.

Using $\sin\phi \approx H/L$, the tangential component of the resultant force exerted by gravity in the return side G_r is:

$$G_r = g(\rho_{belt}t_{belt})B|H| \tag{5.6}$$

and in the carrying side

$$G_c = \frac{gC|H|}{U} + G_r \tag{5.7}$$

t_{belt} - belt thickness
ρ_{belt} - belt density

5.4.1 Inclined Conveyor

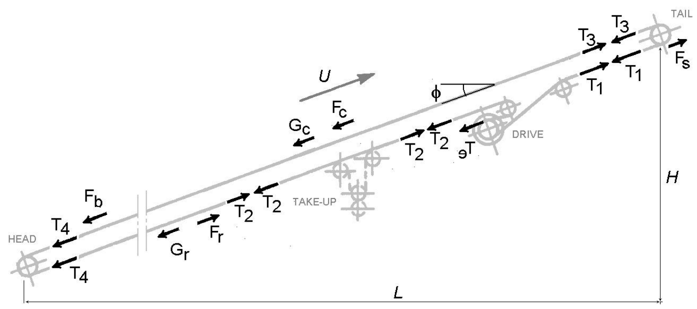

Figure 5.4: Tensions in an inclined conveyor

The set of equations for tensions in the belt, in the case of an inclined conveyor is:

$$\begin{cases} T_1 = T_3 + F_s \\ T_3 = T_4 + F_b + G_c + F_c \\ T_1 = T_e + T_2 \\ T_4 + G_r + F_r = T_2 \end{cases} \tag{5.8}$$

As resultant from the set of equations, the effective tension T_e is:

$$T_e = G_c + F_b + F_c + F_s + F_r - G_r \tag{5.9}$$

5.4.2 Declined Conveyor

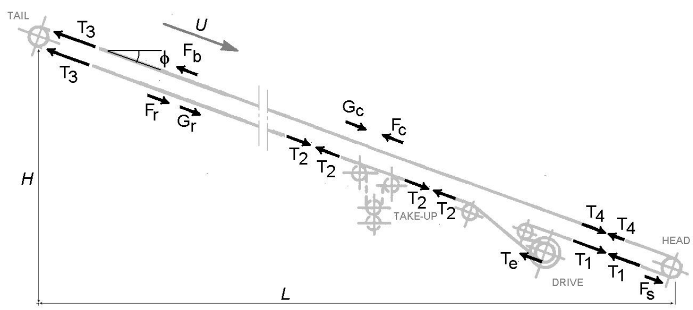

Figure 5.5: Tensions in a declined conveyor

In the declined conveyor the set of equations is:

$$\begin{cases} T_1 = T_4 + F_s \\ T_1 = T_e + T_2 \\ T_4 + G_c = F_b + F_c + T3 \\ T_3 = T_2 + F_r + G_r \end{cases} \tag{5.10}$$

The effective tension is:

$$T_e = G_r + F_b + F_c + F_s + F_r - G_c \tag{5.11}$$

5.4.3 Declined Conveyor with Regenerative Load

The set of equations for tensions in the belt is:

$$\begin{cases} T_1 + F_b + F_c = G_c + T_4 \\ T_1 = T_e + T_2 \\ T_3 = T_4 + F_s \\ T_2 = F_r + G_r + T_3 \end{cases} \tag{5.12}$$

The effective tension is:

$$T_e = G_c - G_r - F_b - F_c - F_s - F_r \tag{5.13}$$

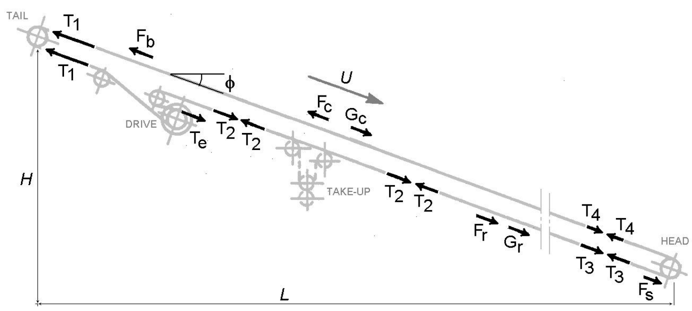

Figure 5.6: Tensions in a declined conveyor with regenerative load

5.4.4 Take-up and Working Tensions

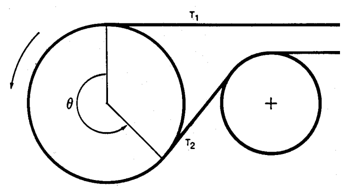

Figure 5.7: Tensions in the belt round a drive pulley

The rope friction law relates the effective tension T_e, tight side tension T_1 and slack side tension T_2:

$$T_2 \geq f_{start} \times \frac{T_e}{e^{\mu_p \theta_p} - 1} \tag{5.14}$$

In the condition above f_{start} is a factor that depends on the drive system and starting procedures, θ_p is the contact angle and μ_p the friction coefficient between pulley and belt.

The slack side tension T_2 is the take-up tension, and its value must be the minimum that keeps condition (5.14), i.e. no slip. It can be increased if theoretical negative tensions exist. The working tension is the maximum tension in the belt loop T_{max}. As the sum of resistances is linear along the conveyor length T_{max} will occur in the extremities or in the loading zone:

$$\begin{cases} T_{max} = \max(T_1, T_3, T_4 + F_b) & \text{Inclined Conveyor} \\ T_{max} = \max(T_1, T_3 + F_b, T_4) & \text{Declined Conveyor} \\ T_{max} = \max(T_1 + F_b, T_3, T_4) & \text{Regenerative Load} \end{cases} \tag{5.15}$$

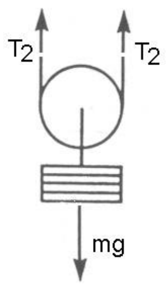

Figure 5.8: Take-up tension

5.5 Belt Selection

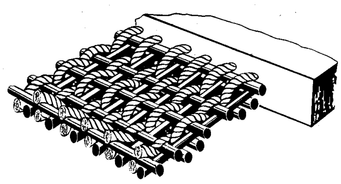

Figure 5.9: Fabric belt carcass

Belt selection is based on the maximum working tension and bulk material properties.

The working tension specify the belt class and strength. Up to certain tensions fabric and solid woven belts are suitable. For higher tensions the most common is the steel cord belt.

Environment conditions and bulk material properties have certain influence to chose the carcass type, referring factors as temperature; but their influence is mostly on the cover, to prevent abrasion and/or corrosion by chemically aggressive materials.

Reference [1] suggest a safety factor of $sf = 10$ on the maximum working tension to specify resistance of fabric belts and $sf = 7.5$ for steel cord belts.

$$sf = \frac{R \times B}{T_{max}} \tag{5.16}$$

The Apex Fenner catalog/guide on conveyor belts, ref. [10], was chosen to be used on belt selection. The belt can be a Nylon-Polyester fabric, to what a rubber or PVC compound should serve as bottom and top cover.

5.6 Support Geometry

The support has a triple utility: as one of the surfaces that form the air bearing, physical support for the belt and load, and duct for the air flow.

Both carrying and return sides can be implemented with air-bearings. For the return side the shape does not need to be the same. As there is no load the trough radius can be higher.

5.6.1 Carrying Side Support Shape

The support must have a trough shape, so that the belt position in the width direction may be stable. A round geometry was selected, due to its simplicity. The following calculations and expressions apply to the carrying side.

Figure 5.10: Support geometry

The cross section area of the bulk material is:

$$A_b = \frac{C}{U \rho_{bulk}} \tag{5.17}$$

A minimum distance between the border and the bulk material must exist in the belt to avoid spillage. It is recommended by ref. [1] that the belt filled width b must be not less than the empirical value:

$$b = 0.9 \times B - 2 \times 0.023 \tag{5.18}$$

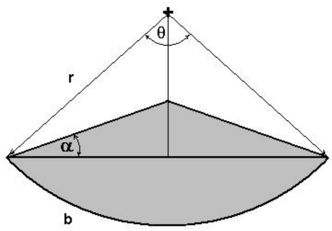

Figure 5.11: Bulk material section

The expression that relates the radius of curvature of the belt r with the bulk material area, shadowed in figure (5.11), is:

$$A_r = \frac{rb}{2} - \frac{r^2}{2}\sin(b/r) + r^2 \sin^2(b/2r)\tan\alpha \tag{5.19}$$

where α is the conveying angle and takes values between 0 and 27° depending on the bulk material .

The radius r is obtained solving:

$$A_b = A_r \Longrightarrow r = f(C, U, \alpha, b, \rho_{bulk}) \tag{5.20}$$

The belt thickness is $t_{belt} \ll r$ and the support radius r_t can be considered $r_t = r$.

5.7 Load Pressure

Average load density ρ_m:

$$\rho_m = \frac{A_r \rho_{bulk} + t_{belt} b \rho_{belt}}{A_r + t_{belt} b} \tag{5.21}$$

The depth of the load is:

$$d(z) = r\left(\cos(\frac{z}{r}) - \cos(\frac{b}{2r}) + \left(\sin(\frac{b}{2r}) - \sin(\frac{z}{r})\right)\sin(\alpha)\right) \tag{5.22}$$

The load $p(z)$ is:

$$p(z) = g\rho_m d(z) \tag{5.23}$$

For the return side, as there is no load, the influence of belt curvature can be significant. If the radius is high one can consider that the pressure changes linearly from center to the border of the belt. With this assumption the pressure at the center is:

$$p_{maxret} = 2 \times g\rho_{belt}t_{belt} \tag{5.24}$$

5.8 Minimum Distance Between Orifices

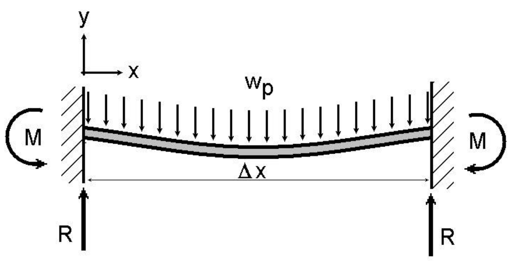

Figure 5.12: Structural model of the belt

The following calculations are useful to verify the distance between orifices. A beam with fixed supports is chosen to model the belt. This assumes a static belt.

From reference [5] the maximum deflection of the beam in figure (5.12) is:

$$y_{max} = \frac{w_p(\triangle x)^4}{384E_xI_x} \tag{5.25}$$

with second moment of area I_x:

$$I_x = \frac{\triangle z t_{belt}^3}{12} \tag{5.26}$$

The load $w[N/m]$ is related to the clearance pressure $p[N/m^2]$ by:

$$w_p = p \times \triangle z \tag{5.27}$$

The minimum distance between orifices is:

$$\triangle x = \sqrt[4]{\frac{32y_{max}E_xt_{belt}^3}{p}} \tag{5.28}$$

The term y_{max} is a fraction of the fluid film thickness. It must be specified using the predicted overload W/W_0 and it is directly derived from expression (4.27):

$$y_{max} = h\sqrt[6]{\frac{1-\beta W/W_0}{(1-\beta)(W/W_0)^2}} \tag{5.29}$$

5.9 Support Thickness

The support thickness l_s is necessary to calculate the losses in the orifices and to have an idea of structural costs. From the support shape in figure (5.13.a) a simplification was taken trough (5.13.b) to (5.13.c).

The corner of the rectangle will have the highest effort. One of the section with length f is modeled with a beam with a distributed load p_s and an axial load of value $e \times p_s/2$. As the goals of this study does not include the final

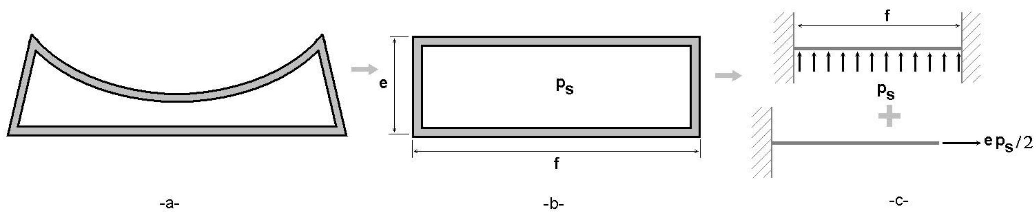

Figure 5.13: Support structure model

definition of the support geometry, the values of the variables e and f can be approximated by:

$$f = B \tag{5.30}$$

and:

$$e = r\left(1-\cos\frac{b}{2r}\right)+0.25 \tag{5.31}$$

The maximum normal stress in the beam is:

$$\sigma = \frac{p_s f^2}{2l_s^2}+\frac{p_s e}{2l_s} \tag{5.32}$$

The maximum shear stress:

$$\tau = \frac{3p_s f}{4l_s} \tag{5.33}$$

The thickness l_s is obtained solving the equation:

$$S_y = 2n_l n_s \sqrt{\frac{\sigma^2}{4} + \tau^2} \Longrightarrow l_s \tag{5.34}$$

where S_y is the yield strength of the support material, n_l and n_s the safety factors for load and material uncertainties.

5.10 Required Flow

Using the concept of hydraulic resistance, expression (4.9) can turn in the form:

$$Q_z = \frac{p_{max}}{R_z} \tag{5.35}$$

with

$$R_z = \frac{12\mu B/2}{h^3 \triangle x} \tag{5.36}$$

where $\triangle x$ is the distance between orifices.

Expression (5.35) is the necessary flow to provide an average fluid film thickness h. It is the flow coming out of the clearance for each side of the belt and per length $\triangle x$. Once the flow is obtained, the local fluid film thickness as a function of the coordinate z is:

$$h_z = \sqrt[3]{\frac{12\mu Q_z}{|\partial p/\partial z| \triangle x}} \tag{5.37}$$

with

$$\partial p/\partial z = g\rho_m \left(-\sin(\frac{z}{r}) - \cos(\frac{z}{r}) \sin(\alpha) \right) \tag{5.38}$$

5.11 Orifice Diameter

The orifice flow Q_i is:

$$Q_i = 2Q_z \tag{5.39}$$

The diameter of the orifices is:

$$d = \sqrt{\frac{8Q_z}{\pi C_d}\left(\frac{\rho}{2(p_s - p_0)}\right)^{1/2}} \tag{5.40}$$

with:

$$C_d = \left(1.5 + 13.74\sqrt{\frac{\mu\pi l}{8Q_z\rho}}\right)^{-1/2} \qquad \text{for}\frac{Q_i\rho}{\mu\pi l} > 12.5 \tag{5.41}$$

$$C_d = \left(2.28 + 64\frac{\mu\pi l}{4Q_i\rho}\right)^{-1/2} \qquad \text{for}\frac{Q_i\rho}{\mu\pi l} < 12.5 \tag{5.42}$$

5.12 Drive and Pumping Power

The drive power is:

$$H_d = T_e \times U \tag{5.43}$$

The pumping power, assuming the same flow source for both the carrying and return side:

$$H_p = p_s(Q_c\frac{L}{\triangle x_c} + Q_r\frac{L}{\triangle x_r}) \tag{5.44}$$

The values of the flow out of the clearance in each side of the belt, per length $\triangle x$, Q_c and Q_r, are obtained using expression (5.35).

5.13 Temperature Rise

In the carrying side the fluid temperature rise is:

$$\triangle T_c = \frac{H_{pc} + UF_c}{Q_{tc}\, c_p\, \rho_{air}} \tag{5.45}$$

The term $H_{pc} + U \times F_c$ is the dissipated power, and Q_{tc} the total flow in the carrying side.

For the return side:

$$\triangle T_r = \frac{H_{pr} + U F_r}{Q_{tr}\, c_p\, \rho_{air}} \tag{5.46}$$